Multicellular PD Control in Microbial Consortia

Vittoria Martinelli, Davide Salzano, Davide Fiore, Mario di Bernardo

***Abstract*— We propose a multicellular implementation of a classical PD feedback controller to regulate gene expression in a microbial consortium. The implementation involves distributing the proportional and derivative control actions between two different cellular populations that can communicate with each other and regulate the output of a third target cellular population. We derive analytical conditions on biological parameters and control gains to adjust the system's static and dynamical properties. We then evaluate the strategy's performance and robustness through extensive *in silico* experiments in BSim, a realistic simulator of bacterial populations.**

I. Introduction

The aim of Synthetic Biology is to engineer biological systems with novel functionalities [1]. This is made possible by designing artificial genetic circuits and embedding them into living cells, such as bacteria or yeast, changing their natural behavior to make them, for example, produce some proteins or other chemicals of interest. Applications range from health treatments [2] to bioremediation [3] and production of drugs or biofuels [4]. However, due to the inherently nonlinear and stochastic nature of the biochemical processes involved, reliable and robust regulation of gene expression must be guaranteed by designing synthetic feedback control architectures, see, e.g., [5], [6] for an overview of the emerging field of *cybergenetics*. To achieve this goal, different solutions have been proposed in the literature; most notably, the antithetic feedback controller realizing an integral action that guarantees robust perfect adaptation with respect to noise and parameters' uncertainties [7], [8]. Recently, it has been proposed that Proportional-Integral-Derivative (PID) controllers can be implemented via biomolecular reactions and embedded in a single cell to enhance the stability and performance of antithetic controllers, by adding both promptness of regulation response and damping with respect to oscillations [9], [10]. However, in some biological applications, in which it is desired to have a quick response without overshoots, an integral action is not required or should be avoided, since it could add oscillations in the closed-loop response that might be undesirable. For example, this is particularly important when engineering the immune response of T-cells [11]. In these cases a simpler PD control scheme should be preferred that, when adequately tuned, can guarantee fast and damped regulation of the biological process without causing the onset of unwanted oscillatory responses.

The implementation of biochemical controllers in living cells is also limited by technological and biological constraints, e.g. incompatible chemical reactions, metabolic load or retroactivity [1]. As a consequence, embedding more complex biomolecular controllers consisting of multiple actions (e.g. a PI, PD or PID) inside a single cell can be challenging. A promising solution to these problems is to distribute the control functionalities across different populations in a microbial consortium of multiple populations. The resulting *multicellular* control architecture can both minimize unwanted effects and increase modularity and re-usability of the designed components, see e.g., [1].

In this letter, we integrate and expand our previous work on multicellular PI controllers [12] by presenting a multicellular PD control strategy where two *controller populations*, each implementing one of the two control actions, regulate a biological process inside a third *target population*, closing the feedback loop by means of diffusing quorum sensing molecules produced by the cells. We derive a model of the consortium and obtain analytical conditions on the control parameters that can be employed to tune the static and dynamical responses of the closed-loop system. The theoretical analysis is complemented with exhaustive *in silico* experiments carried out via the realistic agent-based microbial simulation platform *BSim* [13].

II. Multicellular PD control strategy

As stated above, the overarching goal of our design is to engineer a multicellular consortium of three cellular populations, two controller populations and a target population; the former implementing a proportional and derivative control action, respectively, in order to tame the output of some biological process of interest embedded within the latter. The aim is for the biomolecular controller populations to realize a strategy similar to the classical PD control strategy [14],

$$u_{PD}(t) := u_P(t) + u_D(t) = k_P e(t) + k_D \dot{e}(t), \qquad (1)$$

where $k_P > 0$ and $k_D > 0$ are the proportional and derivative gains, $e(t)$ is the control error defined as the mismatch between the measured output, say $y(t)$ of the process within the target population and the desired reference value $Y_{\mathrm{d}}(t)$,

Vittoria Martinelli and Mario di Bernardo are with the Department of Electrical Engineering and Information Technology, University of Naples Federico II, Via Claudio 21, 80125 Naples, Italy (email: vittoria.martinelli@unina.it). Mario di Bernardo is also with the SSM - School for Advanced Studies, Naples, Italy (email: mario.dibernardo@unina.it). Davide Salzano is with the Department of chemical. materials and industrial production engineering, University of Naples Federico II, Piazzale V. Tecchio 80, 80125, Naples, Italy (email: davide.salzano@unina.it). Davide Fiore is with the Department of Mathematics and Applications "R. Caccioppoli", University of Naples Federico II, Via Cintia, Monte S.Angelo, 80126 Naples, Italy (email: davide.fiore@unina.it).

The authors wish to acknowledge support from the research project PRIN 2017 - VECTORS funded by the Italian Ministry of University and Research, the Italian PNRR Research project MNESYS and the Italian PNC Research project "Digital Health".

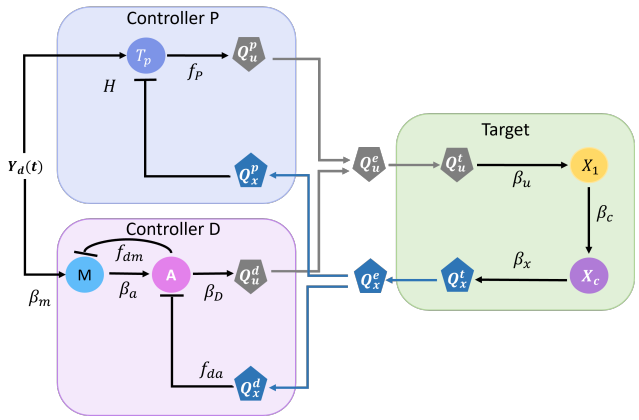

Fig. 1: Abstract implementation of the proposed multicellular PD controller. The controller populations compare the reference signal $Y_{\mathrm{d}}(t)$ and the quorum sensing molecule Q_x, which is produced proportionally to the target gene X_c. The process $\Phi(t)$ is represented by the couple of genes X_1 and X_c, in which X_1 is the actuated by the quorum sensing molecule Q_u. Circles represent internal molecular species, while polygons are the signaling molecules.

provided either externally to the controller cells or hard-coded into them as a constitutive promoter. As in [9], here we assume that the desired output, $Y_{\mathrm{d}}(t)$ is either a succession of step functions or some constant value.

The abstract biological implementation of our proposed distributed PD control strategy is shown in Figure 1. Therein, each controller population computes the control error $e(t)$ by comparing the reference signal $Y_{\mathrm{d}}(t)$ with the measure of the output $y(t)$ corresponding to the expression level of X_c within the target population. Such measure is broadcast to the whole consortium via the quorum sensing molecule Q_x which acts as a proxy for $y(t)$. The control input $u_{PD}(t)$ computed by the two controller populations is delivered to the target cells by means of the quorum sensing molecule Q_u, that is produced by the controllers and effectively serves as the "actuating" signal in this multicellular control scheme. To avoid cross-talking effects [15], Q_x and Q_u are assumed to be orthogonal.

We will show next via mathematical modeling that the biomolecular reactions embedded in each cell populations and depicted in Figure 1 implement the biological equivalent of a distributed PD controller.

A. Mathematical Modelling

We derive a model capturing the *aggregate* dynamics of the microbial consortium, that is the evolution of the concentrations of the biochemical species averaged over all cells in a populations. (Details on the derivation of the aggregate dynamics from the single cell dynamics are reported in Appendix C.)

As also done in [12], we make the following simplifying assumptions: (i) all populations in the consortium are equally balanced, that is, the three populations are composed by the same number of cells, N; (ii) the total number of cells in the consortium is constant. Note that the former assumption can be achieved by means of external ratiometric controllers, e.g. [16], while the latter assumption is generally verified in experimental environments with limited space and resources, e.g., microfluidics, chemostats, vials. From these assumptions it follows that the diffusion dynamics of the quorum sensing molecules through the cells' membranes can be supposed to have the same diffusion rate η. (This assumption will be relaxed later in the *in silico* experiments reported in Section IV where we will take into account cell-to-cell variability and other more realistic spatio-temporal effects.) In what follows, the superscripts e, t, p, d, are used to denote quantities in the "environment", in the "target" cells, in the "proportional", or in the "derivative" controller cells, respectively.

1) Target cells: As done in [7], [9], we assume here that the biological process to be controlled inside the target cells consists of only two genes, X_1 and X_c (Figure 1). The target gene X_c is directly activated by X_1, which in turns is actuated by the quorum sensing molecule Q_u produced by the controller cells. Using mass-action kinetics, the dynamics of the genetic network inside the target cells can therefore be described by the following set of ODEs:

$$\begin{aligned} \dot{X}_1 &= \beta_u Q_u^t - \gamma_1 X_1, \\ \dot{X}_c &= \beta_c X_1 - \gamma_c X_c, \end{aligned} \tag{2}$$

where β_u and β_c are activation rates describing the strength of the transcription factors X_1 and Q_u, while γ_1 and γ_c are the degradation rates of X_1 and X_c, respectively.

The output of the process, corresponding to the expression level of X_c, is broadcast to the other cells by means of the diffusing quorum sensing molecule Q_x, which is produced by the target cells. Assuming as in [12] that the production of Q_x is proportional to X_c, the dynamics of the sensing molecule inside the target cells is described by:

$$\dot{Q}_x^t = \beta_x X_c + \eta(Q_x^e - Q_x^t) - \gamma_t Q_x^t, \tag{3}$$

where β_x is the activation rate of Q_x, η is the diffusion rate of the molecule across the cell membrane, and γ_t is the dilution rate into the target cells.

2) Proportional controller cells: The Proportional controller is implemented here as in [9] as a nonlinear function $f_P = f_P(Q_x, Y_{\mathrm{d}})$, activating the production of Q_u. Specifically, the dynamics of the concentration of Q_u in the Proportional controllers is given by:

$$\dot{Q}_u^p = \beta_P Y_{\mathrm{d}} \frac{\mu Y_{\mathrm{d}}}{\mu Y_{\mathrm{d}} + \theta Q_x^p} + \eta(Q_u^e - Q_u^p) - \gamma_p Q_u^p, \tag{4}$$

where γ_p is the dilution rate of the quorum sensing molecules into the Proportional cells, μ and θ are positive control parameters, and β_P is a tunable parameter which plays the role of a proportional gain. It has been shown in [9] that the first term in (4) realizes a control action that is a function of the control error:

$$e(t) := \mu Y_{\mathrm{d}} - \theta Q_x. \tag{5}$$

3) Derivative controller cells: Biomolecular topologies allowing cells to sense temporal changes of molecules signals [17], [18] can be employed to realize a derivative control action. As shown in Appendix A, an approximation of the time derivative of the control error $e(t)$ can be obtained by embedding in the controller population the biomolecular circuit represented in Figure 1, whose dynamics can be described as follows:

$$\begin{aligned} \dot{A} &= \beta_a M - \gamma_a Q_x^d \frac{A}{k_a + A} - \gamma_d A, \\ \dot{M} &= \beta_m Y_{\mathrm{d}} - \gamma_m A \frac{M}{k_m + M}, \end{aligned} \tag{6}$$

where γ_d is the dilution rate of A due to cell growth and division, and β_a and β_m are activation rates of species A and M, respectively, which in turns are actively degraded by Q_x and A, respectively, through enzymatic reactions modeled here with Michaelis-Menten functions with constants γ_a, k_a, γ_m, k_m. For the sake of simplicity, we assumed here that the quorum sensing molecule Q_x also directly acts as a degradation enzyme on A. The derivative control action is then delivered to the targets by means of the quorum sensing molecule Q_u, produced by the controllers at a rate proportional to A (and thus proportional to an approximation of $\dot{e}(t)$), whose concentration inside the controllers is given by:

$$\dot{Q}_u^d = \beta_D A + \eta(Q_u^e - Q_u^d) - \gamma_d Q_u^d, \tag{7}$$

where β_D plays the role of a derivative gain, and the other parameters have an analogous meaning to those in (3).

In addition, the dynamics of Q_x and Q_u into cells where they are not produced is described by:

$$\begin{aligned} \dot{Q}_x^{\mathrm{h}} &= \eta(Q_x^e - Q_x^{\mathrm{h}}) - \gamma_h Q_x^{\mathrm{h}}, \quad \mathrm{h} \in \{p, d\} \\ \dot{Q}_u^t &= \eta(Q_u^e - Q_u^t) - \gamma_t Q_u^t. \end{aligned} \tag{8}$$

Finally, the model is completed by describing the evolution of the concentration of the quorum sensing molecules into the environment:

$$\begin{aligned} \dot{Q}_x^e &= N\eta \sum_{\mathrm{j} \in \mathcal{S}} (Q_x^{\mathrm{j}} - Q_x^e) - \gamma_e Q_x^e, \\ \dot{Q}_u^e &= N\eta \sum_{\mathrm{j} \in \mathcal{S}} (Q_u^{\mathrm{j}} - Q_u^e) - \gamma_e Q_u^e, \end{aligned} \tag{9}$$

where N is the number of cells in each population (assumed to be balanced), and $\mathcal{S} = \{p, d, t\}$.

III. Analysis and Gain Tuning

We will show next that, as for the classical PD control, the addition of the derivative action to the consortium can provide a prompter and better regulation of the process output inside the target cells. However, the control gains β_P and β_D in (4) and (7) need to be appropriately tuned to achieve the desired stability and performance. After presenting a reduced model of the closed-loop system, in this section we provide analytical conditions on the control gains that can be used to tune the static precision and the characteristics of the transient response, and we compare them to those of the simpler Proportional controller presented in [12]. Later we will numerically investigate the effect of parameters' uncertainties on the performance of the closed-loop system.

A. Reduced order model

To derive meaningful analytical relationships between the dynamical properties of closed-loop system and the control gains, we make the following simplifying assumptions, commonly made in the literature, e.g., [9], [12], [19].

Assumptions *The multicellular control system* (2)-(9) *satisfies the following proprieties:*

- A1 *All cell populations grow and divide at the same rate.*
- A2 *The quorum sensing molecules Q_u and Q_x diffuse faster than they degrade.*
- A3 *The enzymatic reactions in* (6) *occur with saturation of the substrates.*
- A4 *The dynamics of the derivative action* (6) *is sufficiently faster than the controlled process in* (2).

Under the previous assumptions, the dynamics of the multicellular system can be approximated by the following reduced order model (see Appendix A for the detailed derivation), with A defined as in (20):

$$\begin{aligned} \dot{X}_1 &= -\gamma_1 X_1 + \frac{1}{3\gamma}\beta_u \left(\beta_P Y_{\mathrm{d}} \tfrac{3\gamma\mu Y_{\mathrm{d}}}{3\gamma\mu Y_{\mathrm{d}} + \theta\beta_x X_c} + \beta_D A\right), \\ \dot{X}_c &= \beta_c X_1 - \gamma X_c. \end{aligned} \tag{10}$$

Remark 1 *Assumption A1 implies that all species have the same dilution rate, i.e. $\gamma_1 = \gamma_c = \gamma_p = \gamma_d = \gamma_t = \gamma$. Assumption A2 requires that $\eta \gg \Gamma_{PD}$, with $\Gamma_{PD} := \gamma_p + \gamma_d + \gamma_t + \gamma_e = 3\gamma + \gamma_e$. Assumption A3 implies that $K_a \ll A$ and $K_m \ll M$ [20]. Assumption A4 can be satisfied by requiring that the frequency content of $X_c(t)$ (and thus of $Q_x(t)$) is bounded by some value $\omega_{\max}$, and the parameters of the derivative motif are chosen accordingly (see [9] and Appendix A for details).*

B. Static and transient performance

Setting $\dot{X}_1 = 0$ and $\dot{X}_c = 0$ in (10) we can obtain the equilibrium point (assumed to be positive and locally stable) and compute the control error at steady-state using (5) (the derivation is omitted here for the sake of brevity). We then find that if the control gains are positive ($\beta_P, \beta_D \geq 0$) and such that:

$$\beta_D + \frac{\beta_P}{2}\frac{\gamma_m}{\beta_m} - \frac{9\gamma^4\gamma_m\mu}{\beta_c\beta_u\beta_x\beta_m\theta} = 0. \tag{11}$$

the steady-state error can theoretically be made null provided that all parameters are perfectly known. In practice, this is unrealistic in biological implementations of the controller and therefore the error can only be made small enough by appropriately tuning the gains around the values suggested in (11).

Next, we assess the (local) transient performance by studying the eigenvalues of the linearization of system (10)

about the equilibrium point $(\bar{X}_1, \bar{X}_c)$, with $\bar{X}_c = \frac{\Gamma_{PD}}{\beta_x}\frac{\mu Y_\mathrm{d}}{\theta}$, where $e_\infty = 0$. Simple algebraic manipulations yield:

$$\lambda_{PD_{1,2}} = -\alpha \pm \sqrt{\alpha^2 - \left(\gamma^2 + \frac{\beta_P \beta_c \beta_u \beta_x \theta}{36\gamma^2 \mu}\right)} \tag{12}$$

where $\alpha := \gamma + \frac{\beta_D \beta_c \beta_u \beta_x \gamma_a}{18\beta_a \gamma^2 \gamma_m}$.
The eigenvalues are therefore both real and negative if:

$$\beta_D \geq 18\frac{\beta_a \gamma^3 \gamma_m}{\beta_c \beta_u \beta_x \gamma_a}\left(\sqrt{1 + \frac{\beta_P \beta_c \beta_u \beta_x \theta}{36\gamma^4 \mu}} - 1\right), \tag{13}$$

and correspondingly the transient response is characterized by the absence of oscillations, or complex conjugates with negative real parts otherwise.

C. Comparison with the Proportional controller

To highlight the advantages of adding a derivative control action to the multicellular control scheme, we compare the static and transient performance of the PD controller with that of the P controller alone we previously studied in [12].

Regarding the steady-state, also in the case when only a proportional biomolecular controller is present, the error can be made theoretically null (and therefore closer to zero in practice) provided all the system parameters are perfectly known and the proportional gain is selected about the value:

$$\beta_P^* = \frac{8\gamma^4 \mu}{\beta_c \beta_u \beta_x \theta}. \tag{14}$$

Following similar steps as those taken to obtain (12), we find that in the absence of the derivative action the transient response is governed by the pair of complex conjugate eigenvalues:

$$\lambda_{P_{1,2}} = -\gamma \pm j\sqrt{\frac{\beta_P \beta_c \beta_u \beta_x \theta}{16\gamma^2 \mu}}. \tag{15}$$

Thus, when the derivative action is added to the consortium, if the gains are tuned so that $\lambda_{PD_{1,2}}$ are real, i.e. condition (13) holds, by comparing (12) with (15) we find that the PD strategy can indeed guarantee faster convergence (that is, $|\Re\{\lambda_{P_{1,2}}\}| < \max_i |\Re\{\lambda_{PD_i}\}|$) by further requiring that:

$$\beta_D < \beta_P \frac{\beta_a \gamma_m \theta}{4\gamma\gamma_a \mu}. \tag{16}$$

Also, if $\lambda_{PD_{1,2}}$ are complex conjugate, it is easy to verify that $\Re\{\lambda_{PD}\} < \Re\{\lambda_P\}$ and $\Im\{\lambda_{PD}\} < \Im\{\lambda_P\}$ for any choice of the control gains, therefore, the PD controller guarantees faster response and more damped oscillations than the Proportional controller alone.

IV. In silico Experiments

We validated the proposed distributed PD multicellular architecture via *in silico* experiments carried out in Matlab and BSim [13].

First, we validated the theoretical predictions using Matlab. Specifically, as reported in Figure 2, we computed for different values of the gains β_P and β_D the overshoot $s_\%$, the 5% settling time $T_{s_{5\%}}$, and the relative percentage steady-state error defined as:

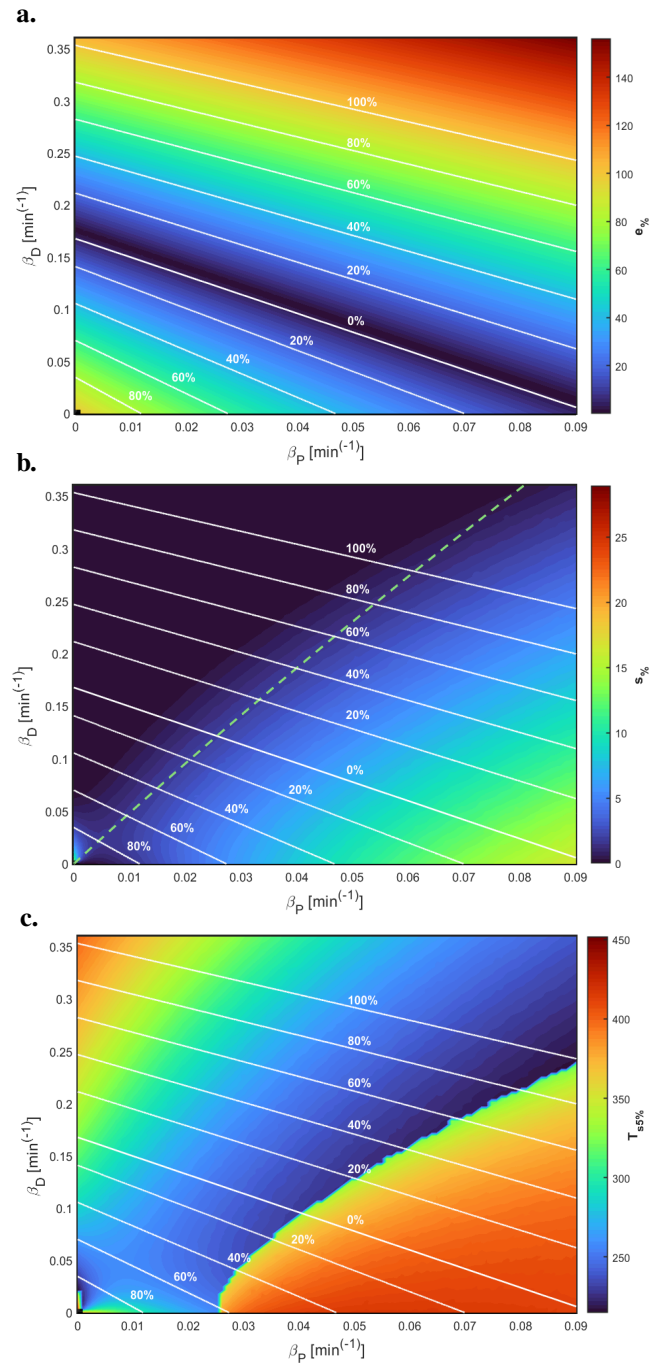

Fig. 2: *In silico* experiments in Matlab: percentage error $e_\%$ (a), percentage overshoot $s_\%$ (b) and settling time $T_{s_{5\%}}$ (c) when the targets are controlled by the PD controller. The control gains β_P and β_D were varied in the intervals $[0, 0.09]$ and $[0, 0.36]$ with step size equal to $0.0009\,\mathrm{min}^{-1}$ and $0.0036\,\mathrm{min}^{-1}$, respectively. The reference signal was set to $Y_\mathrm{d} = 60\,\mathrm{nM}$ in all simulations. The white isoclines bound the regions in the parameters' space (β_P, β_D) with the same upper bound on the percentage error. The 0% isocline in panel (a) is the analytical estimate given by (11) while the green dashed line in panel(b) represents the condition to have real eigenvalues given by equation (13).

$$\bar{e}_\% = \left|\frac{\bar{Q}_x^t - Q_\mathrm{d}}{Q_\mathrm{d}}\right| \times 100\%, \tag{17}$$

where $\bar{Q}_x^t$ is the steady-state value of $Q_x^t(t)$ and $Q_\mathrm{d} = \frac{\mu Y_\mathrm{d}}{\theta}$. We found that, as expected from the analysis, the

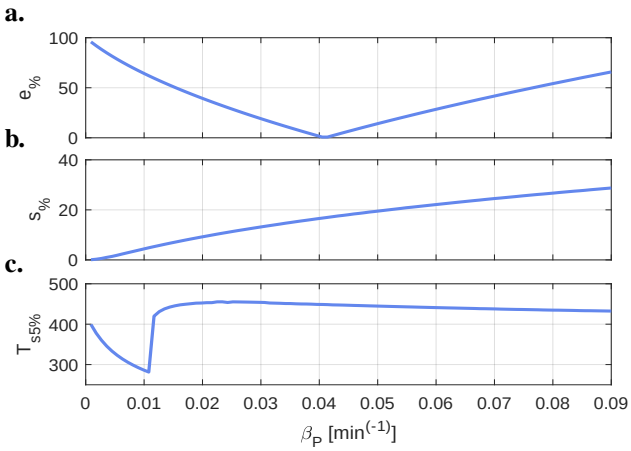

Fig. 3: Proportional performance validation in Matlab: percentage error $e_{\%}$ (a), percentage overshoot $s_{\%}$ (b) and settling time $T_{s_{5\%}}$ (c) when the targets are controlled by a proportional controller. The control gain was varied in the interval $[0, 0.09]$ with step size equal to $0.0009\,\mathrm{min}^{-1}$. The reference signal was set to $Y_{\mathrm{d}} = 60\,\mathrm{nM}$ in all simulations.

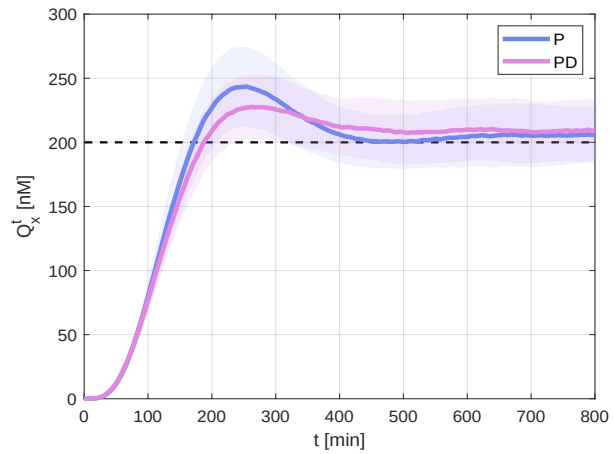

Fig. 4: Control performance validation in BSim: mean (continuous line) and standard deviation (shaded area) of the average concentration of Q_x^t in the targets. The statistics were computed over 10 simulations. The blue lines are obtained using a Proportional controller and the purple ones using a PD controller. Control gains were drawn with uniform distribution from the region of the parameter space (β_P, β_D) in Figure 2 in which $\bar{e}_{\%} < 20\%$. For the PD architecture we also imposed condition (16). The reference signal $Q_{\mathrm{d}} = \mu Y_{\mathrm{d}}/\theta$ is depicted as a dashed line. At $t = 0\,\mathrm{min}$, 18 cells, equally divided between the populations, were positioned at the center of the chamber along a horizontal stripe.

PD strategy can guarantee bounded steady-state error for gains chosen close to the theoretical estimates reported in (11) ($\beta_D < 0.17$, $\beta_P = 0.09 - 0.54\,\beta_D$). For the sake of completeness we also report in Figure 3 the steady-state error, overshoot and settling time when only the Proportional control action is present ($\beta_D = 0$). Also we notice that, as predicted by (12) and (15), the proportional action used on its own always causes overshoots in the closed-loop response whereas there is a wide range of control parameters where the PD action ensures no overshoot. Also, when condition (16) holds ($\beta_D < 4.89\,\beta_P$), the PD architecture provides faster dynamic regulation than the Proportional one.

We further validated our theoretical results by carrying out agent-based simulations in BSim accounting for cell growth, cell-to-cell variability, diffusion and the geometry of cells and of the hosting chamber. In all the simulations, we set the initial concentration for all chemical species to zero. This emulates an experimental protocol where each cellular population is grown separately from the others prior to the beginning of the experiment. We assumed the cells are growing in a scaled-down version of the microfluidic chamber used in [16], [21]. Specifically, the chamber has dimensions $17\mu\,\mathrm{m} \times 15\mu\,\mathrm{m} \times 1\ \mu\mathrm{m}$ and can host around 100 cells, which is a good compromise between computational time and statistical relevance. Unless otherwise stated, the growth and mechanical parameters of cells and the nominal values of the parameters in the network were chosen as described in Appendix B.

We chose values of the control gains β_P and β_D that were shown in Matlab (see Figure 1) to guarantee $e_\infty < 20\%$ when $Y_{\mathrm{d}} = 60\,\mathrm{nM}$ and to also satisfy condition (16). We ran 10 agent-based simulations, each time randomly selecting the control gains with uniform distribution and evaluating the performance. Figure 4 shows that both the P and PD architectures have good regulation capabilities. Moreover, it confirms that on average the addition of a derivative action consistently reduces the overshoot (9.76% for the PD, and 18.29% for the P controller). Instead, the reduction of the settling time was just about 10% (about 355 min for the PD, and 392 min for the Proportional). As for the steady-state error (4.55% for the PD, and 2.71% for the Proportional), the difference between the two strategies was negligible.

Finally, we tested the robustness of the P and PD strategies as the cell-to-cell variability increases in the cell populations. We modeled this effect by drawing, at cell division, each parameter of the daughter cells, say ρ, from a normal distribution centered at its nominal value $\hat{\rho}$ with standard deviation $\sigma = CV \cdot \hat{\rho}$, where CV is the coefficient of variation. We compared the robustness of the two architectures, as the CV increases, by evaluating the settling time, the overshoot, and the average relative percentage steady-state error, defined as

$$e_{\%} = \frac{1}{n} \sum_{k=1}^{n} \left| \frac{\hat{Q}_x^t - Q_{\mathrm{d}}}{Q_{\mathrm{d}}} \right| \times 100\%, \tag{18}$$

where $\hat{Q}_x^t$ is the value of $Q_x^t(t)$, averaged over the last 200 min, of the k-th experiment, $Q_{\mathrm{d}} = \frac{\mu Y_{\mathrm{d}}}{\theta}$, and n is the total number of experiments we conducted for each value of CV. Figure 5 shows that the P and the PD strategies both possess good robustness (the steady-state error never exceeds 20%). We observe that while the Proportional controller seems to guarantee a lower residual error under perturbations [Figure 5(a)], the PD control strategy reduces the overshoot even in the presence of high cell-to-cell variability [Figure 5(c)]; no significant difference between the two being detected in terms of settling time [Figure 5(b)].

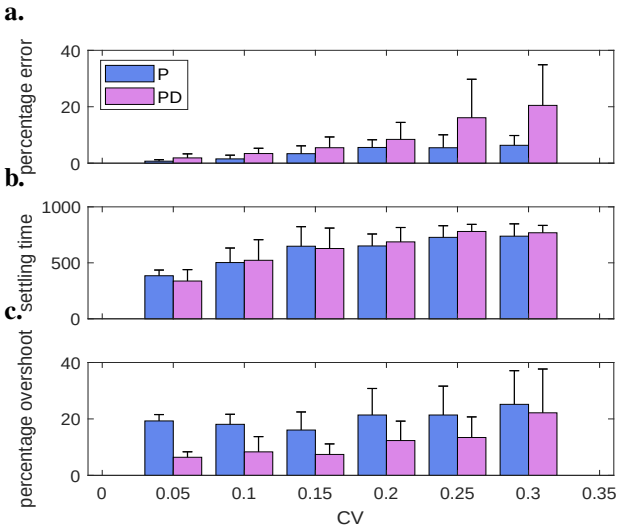

Fig. 5: Sensitivity to parameter variations: mean and standard deviation of the percentage of error at steady-state (a), settling time (b) and overshoot (c) as the cell-to-cell variability increases. Blue bars are obtained using only a Proportional controller and purple bars when a PD controller was employed. For each value of $CV \in \{0.05, 0.1, 0.15, 0.2, 0.25, 0.3\}$ we performed $n = 50$ simulations drawing independently cells' parameters from a normal distribution centered at their nominal value $\hat{\rho}$ with standard deviation $\sigma = CV \cdot \hat{\rho}$. The reference signal was set to $Y_{\mathrm{d}} = 60\,\mathrm{nM}$, while the gains were chosen as $\beta_P = 0.0414\,\mathrm{min}^{-1}$ and $\beta_D = 0.0933\,\mathrm{min}^{-1}$. All simulations were performed for a total time of $800\,\mathrm{min}$.

V. Conclusions

We discussed the implementation of a distributed biomolecular PD controller, where two cell populations generate proportional and derivative control actions to regulate the output of a process in a third cellular population. Analytical conditions were derived for control gains to achieve a desired performance. It was showed that the derivative action helps reduce overshoots and settling time. Numerical and *in silico* experiments were conducted to confirm the effectiveness of the proposed strategy, despite cell-to-cell variability and other realistic effects. Future work includes adding an integral control action in the consortium to improve the robustness of the strategy and achieve a fully distributed biomolecular PID controller.

Appendix

A. Derivation of the reduced order model (10)

Under Assumption A2, we can assume that the quorum sensing molecules are always at steady state. Therefore, by imposing that $\dot{Q}^j_{\mathrm{h}} = 0$ and $\dot{Q}^e_{\mathrm{h}} = 0$, with $\mathrm{h} \in \{u, x\}$ and $j \in \mathcal{S}$, where $\mathcal{S} = \{t, p, d\}$, and under the hypothesis of a large number of cells, after some algebra we have that:

$$\begin{aligned} Q^j_x &\approx Q^e_x = Q_x = \frac{1}{3\gamma}\beta_x X_c, \\ Q^j_u &\approx Q^e_u = Q_u = \frac{1}{3\gamma}\left(\beta_P Y_{\mathrm{d}} \tfrac{\mu Y_{\mathrm{d}}}{\mu Y_{\mathrm{d}} + \theta Q_x} + \beta_D A\right). \end{aligned} \tag{19}$$

Now, under Assumption A4 there exists some $\omega_{\max}$ upper bounding the frequency contents of $Q_x(t)$, therefore, if the parameters of the derivative motif are chosen so to satisfy the condition $\beta_a\gamma_m \gg |\omega^2_{\max} + \gamma_0\omega_{\max}|$, then A is an approximation of the derivative of the control error $e(t)$ given as (see [9] for further details):

$$A \approx -\frac{1}{3\gamma}\frac{\gamma_a\beta_x}{\beta_a\gamma_m}\dot{X}_c + \frac{\beta_m}{\gamma_m}Y_{\mathrm{d}}. \tag{20}$$

Combining equations (19) and (20) with (2) we finally obtain the reduced model (10).

B. Nominal biochemical parameters

The growth and mechanical parameters used in the BSim simulations were selected as in [19], while the nominal biochemical parameters were chosen as: $\beta_u = 0.06\,\mathrm{min}^{-1}$, $\beta_x = 0.03\,\mathrm{min}^{-1}$, $\gamma = 0.023\,\mathrm{min}^{-1}$, $\eta = 2\,\mathrm{min}^{-1}$ (taken from [19]); $\beta_c = 0.1\,\mathrm{min}^{-1}$, $\mu = 1\,\mathrm{min}^{-1}$, $\theta = 0.3\,\mathrm{min}^{-1}$, $\beta_a = 1.5\,\mathrm{min}^{-1}$, $\beta_m = 0.4167\,\mathrm{min}^{-1}$, $\gamma_a = \gamma_m = 1.5\,\mathrm{min}^{-1}$ (taken from [9]); $\gamma_e = 0.0023\,\mathrm{min}^{-1}$.

C. Derivation of the aggregate model

Here we present the derivation of the aggregate model reported in Section II-A that describes the evolution of the average concentrations of chemical species in the whole consortium. For the sake of brevity, we report there only the case of a consortium comprising Proportional controller cells and target cells. The case of three populations, in which also the derivative controller population is present, follows straightforwardly. The aggregate dynamics of the non-diffusive species (i.e., X_1 and X_c in the target cells, and A and M in the derivative controller cells) follows directly from the single cell model by assuming that the average concentrations follow the same dynamics. For what concerns the diffusive species (i.e., Q_x and Q_u), under the assumptions made in Section III-A, their dynamics inside each cell in the consortium and into the environment is given as (we report here only the dynamics of Q_x for the sake of brevity, a similar analysis follows for Q_u):

$$\dot{Q}^t_{x,k} = \beta_x X_{c,k} + \eta(Q^e_x - Q^t_{x,k}) - \gamma Q^t_{x,k}, \tag{21}$$

$$\dot{Q}^p_{x,i} = \eta(Q^e_x - Q^p_{x,i}) - \gamma Q^p_{x,i}, \tag{22}$$

$$\dot{Q}^e_x = \eta \sum_{\mathrm{j}\in\mathcal{S}} \sum_{k=1}^{N_j} (Q^j_{x,k} - Q^e_x) - \gamma_e Q^e_x, \tag{23}$$

where $X_{c,k}$ and $Q^t_{x,k}$ are the concentrations of the species X_c and Q_x inside the k-th cell of the target population, $Q^p_{x,i}$ is the concentration of the signaling molecule Q_x in the i-th cell embedding the Proportional controller, and Q^e_x is the concentration of Q_x into the environment. Moreover, $\mathcal{S} = \{t, p\}$, and N_t and N_p are the number of cells in the target and Proportional controller populations, respectively. Now, defining $Q^j_x = \frac{1}{N_j}\sum_{k=1}^{N_j} Q^j_{x,k}$ for $j \in \mathcal{S}$ and $X_c = \frac{1}{N_t}\sum_{k=1}^{N_t} X_{c,k}$, we can derive the evolution of the average concentration of Q_x inside each cell population as:

$$\begin{aligned} \dot{Q}^t_x &= \beta_x X_c + \eta(Q^e_x - Q^t_x) - \gamma Q^t_x, \\ \dot{Q}^p_x &= \eta(Q^e_x - Q^p_x) - \gamma Q^p_x. \end{aligned} \tag{24}$$

In addition, we can recast equation (23) as:

$$\dot{Q}_x^e = \eta \sum_{\mathrm{j}\in\mathcal{S}} \left(\sum_{k=1}^{N_j} Q_{x,k}^j - N_j Q_x^e \right) - \gamma_e Q_x^e = \\ = \eta \sum_{\mathrm{j}\in\mathcal{S}} N_j \left(Q_x^j - Q_x^e \right) - \gamma_e Q_x^e, \tag{25}$$

and thus, assuming $N_t = N_p = N$, that is, the two populations are balanced, equation (25) becomes:

$$\dot{Q}_x^e = N\eta \sum_{\mathrm{j}\in\mathcal{S}} (Q_x^{\mathrm{j}} - Q_x^e) - \gamma_e Q_x^e. \tag{26}$$

REFERENCES

[1] D. Del Vecchio, A. J. Dy, *et al.*, "Control theory meets synthetic biology," *Journal of The Royal Society Interface*, vol. 13, no. 120, p. 20160380, 2016.

[2] X. Tan, J. H. Letendre, *et al.*, "Synthetic biology in the clinic: engineering vaccines, diagnostics, and therapeutics," *Cell*, vol. 184, no. 4, pp. 881–898, 2021.

[3] E. L. Rylott and N. C. Bruce, "How synthetic biology can help bioremediation," *Current Opinion in Chemical Biology*, vol. 58, pp. 86–95, 2020.

[4] Y. Yang, T. A. Chaffin, *et al.*, "Plant synthetic biology innovations for biofuels and bioproducts," *Trends in Biotechnology*, 2022.

[5] I. Ruolo, S. Napolitano, *et al.*, "Control engineering meets synthetic biology: Foundations and applications," *Current Opinion in Systems Biology*, vol. 28, p. 100397, 2021.

[6] M. H. Khammash, "Cybergenetics: Theory and applications of genetic control systems," *Proceedings of the IEEE*, vol. 110, no. 5, pp. 631–658, 2022.

[7] C. Briat, A. Gupta, *et al.*, "Antithetic integral feedback ensures robust perfect adaptation in noisy biomolecular networks," *Cell Systems*, vol. 2, no. 1, pp. 15–26, 1 2016.

[8] M. H. Khammash, "Perfect adaptation in biology," *Cell Systems*, vol. 12, no. 6, pp. 509–521, 6 2021.

[9] M. Chevalier, M. Gómez-Schiavon, *et al.*, "Design and analysis of a proportional-integral-derivative controller with biological molecules," *Cell Systems*, vol. 9, no. 4, pp. 338–353.e10, 10 2019.

[10] E. Alexis, L. Cardelli, *et al.*, "On the design of a PID bio-controller with set point weighting and filtered derivative action," *IEEE Control Systems Letters*, vol. 6, pp. 3134–3139, 2022.

[11] P. Wei, W. W. Wong, *et al.*, "Bacterial virulence proteins as tools to rewire kinase pathways in yeast and immune cells," *Nature*, vol. 488, no. 7411, pp. 384–388, 2012.

[12] V. Martinelli, D. Salzano, *et al.*, "Multicellular pi control for gene regulation in microbial consortia," *IEEE Control Systems Letters*, vol. 6, pp. 3373–3378, 2022.

[13] A. Matyjaszkiewicz, G. Fiore, *et al.*, "Bsim 2.0: an advanced agent-based cell simulator," *ACS synthetic biology*, vol. 6, no. 10, pp. 1969–1972, 2017.

[14] K. J. Aström and R. M. Murray, *Feedback Systems. An Introduction for Scientists and Engineers*. Princeton Univ Pr, 2008.

[15] N. Kylilis, Z. A. Tuza, *et al.*, "Tools for engineering coordinated system behaviour in synthetic microbial consortia," *Nature communications*, vol. 9, no. 1, p. 2677, 2018.

[16] D. Salzano, D. Fiore, *et al.*, "Ratiometric control of cell phenotypes in monostrain microbial consortia," *Journal of the Royal Society Interface*, vol. 19, no. 192, p. 20220335, 2022.

[17] E. Alexis, C. C. Schulte, *et al.*, "Biomolecular mechanisms for signal differentiation," *Iscience*, vol. 24, no. 12, p. 103462, 2021.

[18] W. Ma, A. Trusina, *et al.*, "Defining network topologies that can achieve biochemical adaptation," *Cell*, vol. 138, no. 4, pp. 760–773, 8 2009.

[19] D. Fiore, D. Salzano, *et al.*, "Multicellular feedback control of a genetic toggle-switch in microbial consortia," *IEEE Control Systems Letters*, vol. 5, no. 1, pp. 151–156, 2020.

[20] L. Michaelis, M. L. Menten, *et al.*, "Die kinetik der invertinwirkung," *Biochem. z*, vol. 49, no. 333-369, p. 352, 1913.

[21] B. Shannon, C. G. Zamora-Chimal, *et al.*, "In vivo feedback control of an antithetic molecular-titration motif in escherichia coli using microfluidics," *ACS Synthetic Biology*, vol. 9, no. 10, pp. 2617–2624, 2020.